

## Supporting Information

# Microfluidic Mobility Shift Profiling of Lysine Acetyltransferases Enables Screening and Mechanistic Analysis of Cellular Acetylation Inhibitors

*A.W. Sorum, J.H. Shrimp, A.M. Roberts, D.C. Montgomery, N.W. Tiwari, M. Lal-Nag,*

*A. Simeonov, A. Jadhav, and J.L. Meier\**

Chemical Biology Laboratory, National Cancer Institute, Frederick, MD, 21702

### Table of Contents for Supporting Information

	<u>Page</u>
Supporting Figures S1-S8	S2-S7
Supporting Tables S1-S2	S8
Scheme S1: Synthesis of fluorescent peptide substrates	S9
Procedure for KAT coupled-enzyme assay	S10
General synthetic procedures	S11
Synthesis of fluorescent peptide substrates	S11
Synthetic characterization data for fluorescent peptide substrates	S12
References	S13

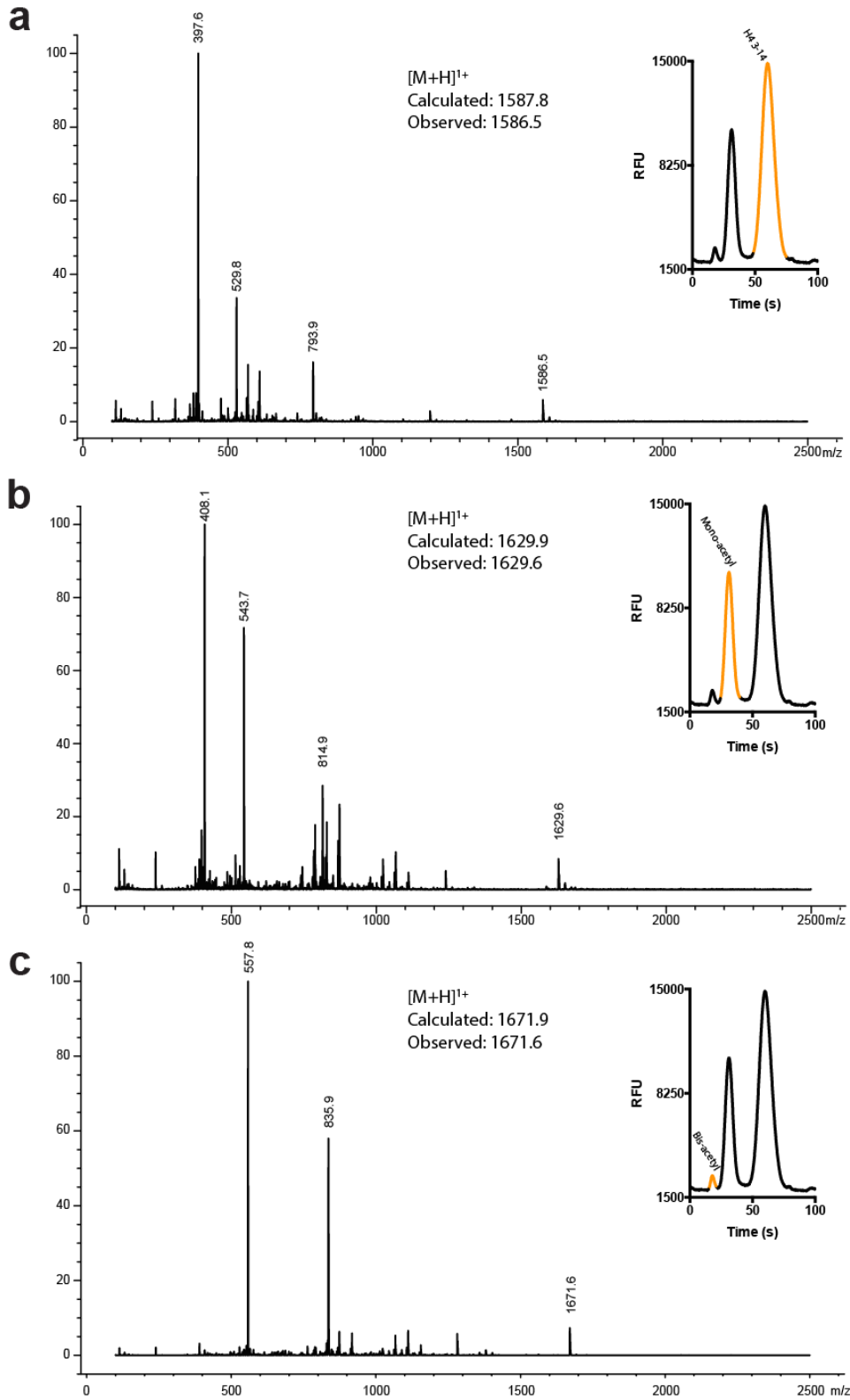


**Figure S1:** LC-MS and microfluidic analysis (inset) of p30 activity with FITC-H4 3-14. (a) LC-MS of non-acetylated starting material corresponding to highlighted peak. (b) LC-MS of mono-acetylated peptide. (c) LC-MS of bis-acetylated peptide. Under conditions of low turnover (0-15%), the bis-acetylated product is not observed (Fig. S2).

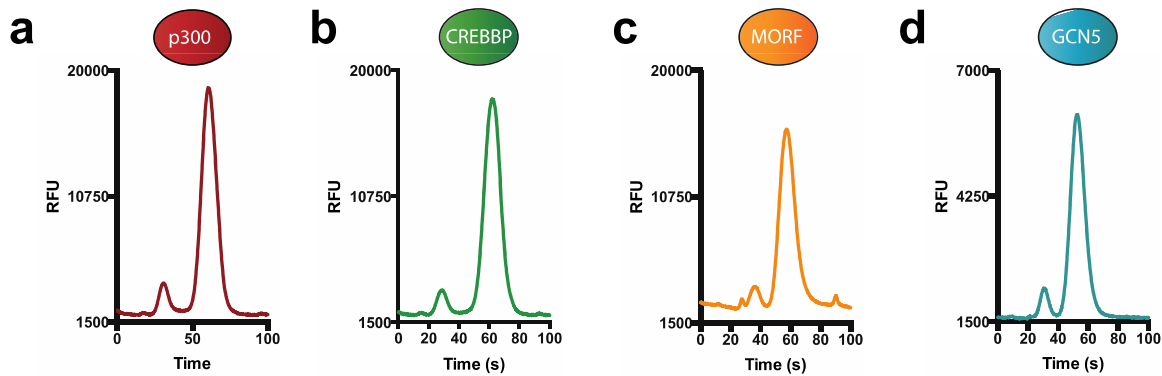


**Figure S2:** Shown are representative chromatograms associated with 10% product turnover. Traces were acquired by addition of Ac-CoA (2.5  $\mu$ M) to reaction buffer with H4 3-14 (5  $\mu$ M) and **(a)** 50 nM p300, **(b)** 150 nM Crebbp or **(c)** 200 nM Morf. **(d)** Gcn5 trace was obtained by addition of Ac-CoA (1  $\mu$ M) to reaction buffer with H3 5-20 (2  $\mu$ M).

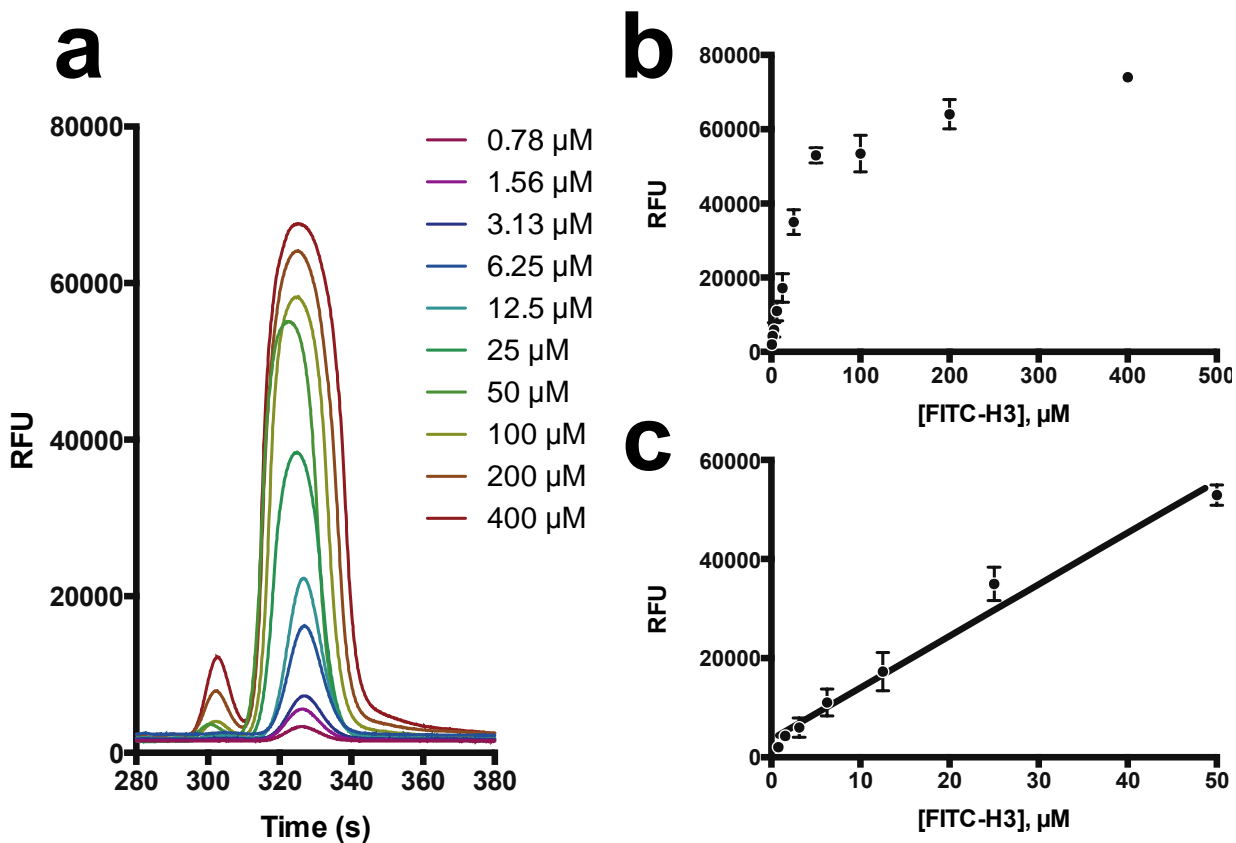


**Figure S3:** Saturation of fluorescence signal at high (> 50  $\mu\text{M}$ ) FITC-peptide substrate concentrations. **(a)** Fluorescence traces of FITC-H3 5-20 at varying concentrations. **(b)** Plot of RFU-values as a function of concentration of FITC-H3. The correlation between RFU and concentration deviates from linearity at concentrations > 50  $\mu\text{M}$ , presumably due to signal saturation. **(c)** Plot of RFU-values depicting the functional (linear) range of FITC-substrate that can be used for KAT assay.

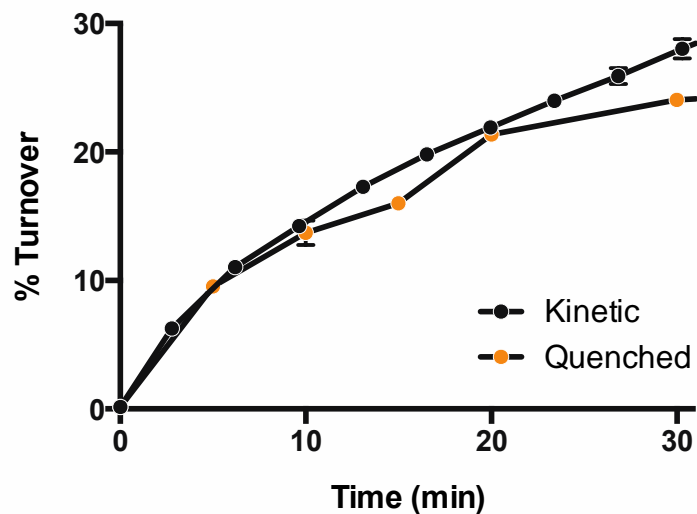


**Figure S4:** Hydroxylamine efficiently quenches KAT-catalyzed reactions. Shown are reaction progress traces for unquenched (kinetic) and quenched reactions. Kinetic samples containing GCN5 and FITC-H3 5-20 were analyzed by microfluidic KAT assay in 3.4-minute intervals following initiation by addition of Ac-CoA. Quenched samples were allowed to proceed for 5, 10, 15, 20 or 30 minutes before addition of hydroxylamine (final concentration 71 mM) to halt reaction progress. These reactions were subsequently analyzed by microfluidic KAT assay to determine the efficiency and stability of the hydroxylamine quench. Error bars represent standard deviation from the mean.

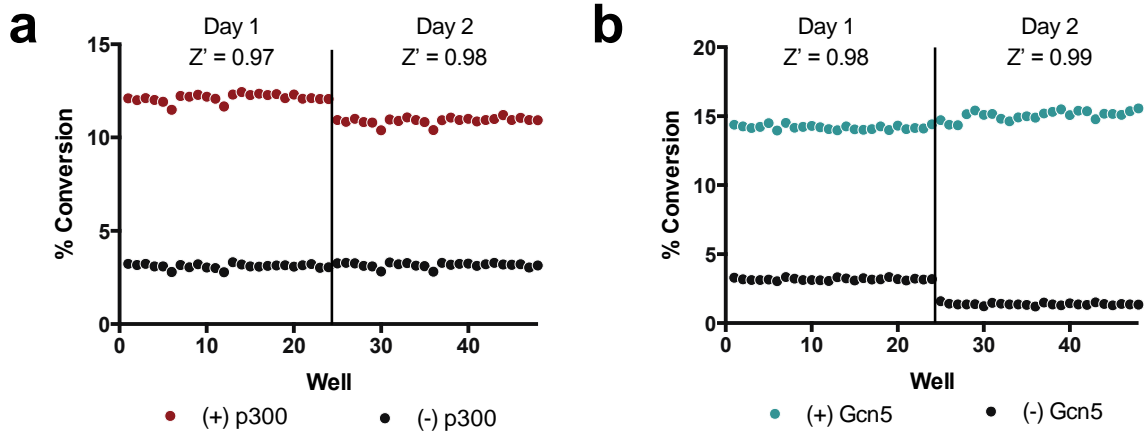


**Figure S5:** Reproducibility of microfluidic KAT assays as assessed using high-to-low controls and day-to-day variability. 24-well replicates of high turnover (with KAT) and low turnover (without KAT) percent-conversion readouts were examined for (a) p300/H4 3-14 and (b) Gcn5/H3 5-20 and are depicted as scatter plots by well number. The average  $Z'$  factor for p300 was determined to be  $0.97_5$  and for Gcn5 was determined to be  $0.98_5$ .

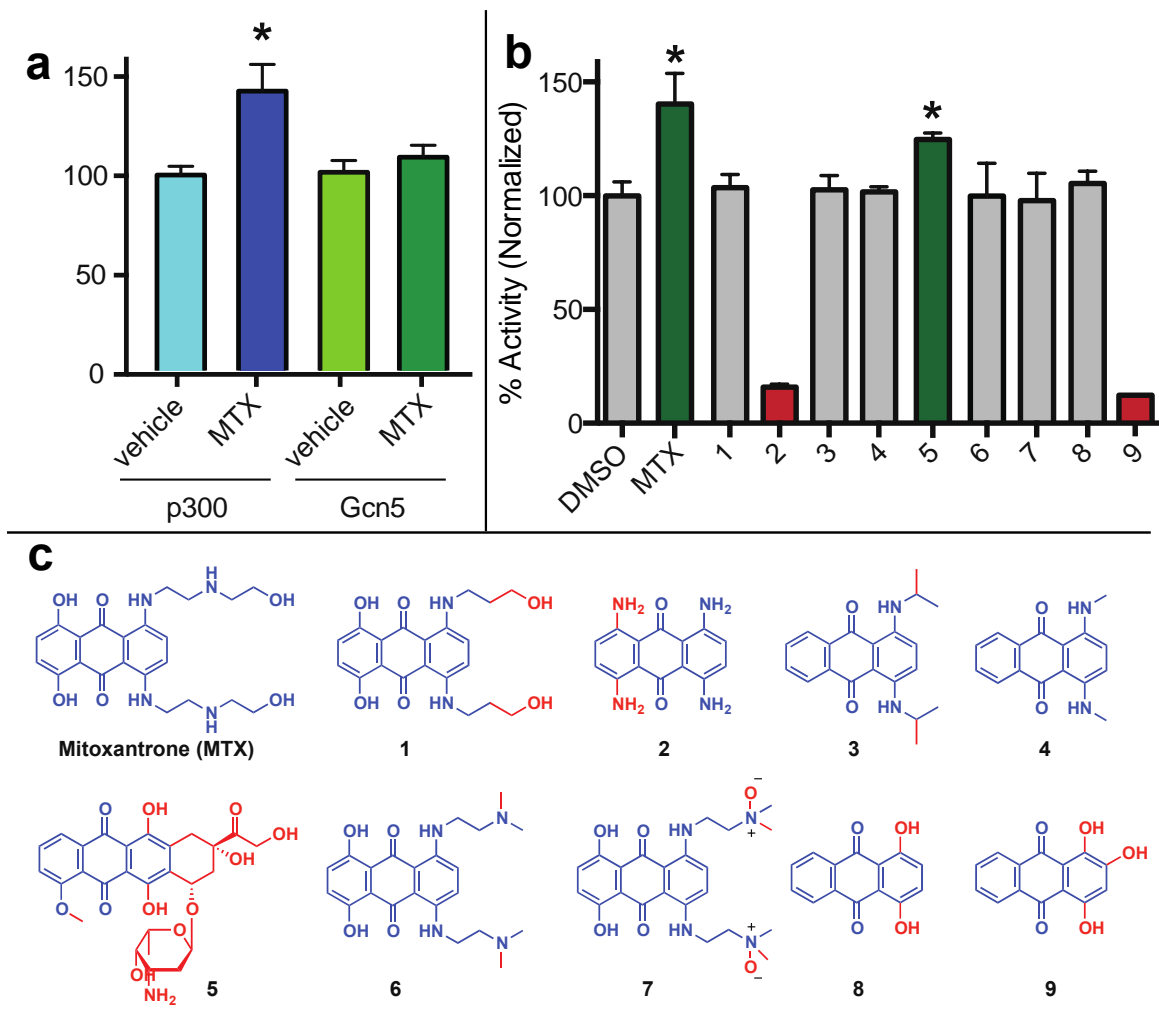


**Figure S6:** Mitoxantrone is a novel p300 activator. (a) Mitoxantrone activates p300 but not Gcn5. (b) Structure-function analysis for activation of p300 by mitoxantrone and related anthraquinones. (c) Structures of analyzed anthraquinones. Blue: structural elements shared with mitoxantrone. Red: Structural elements that diverge with mitoxantrone.

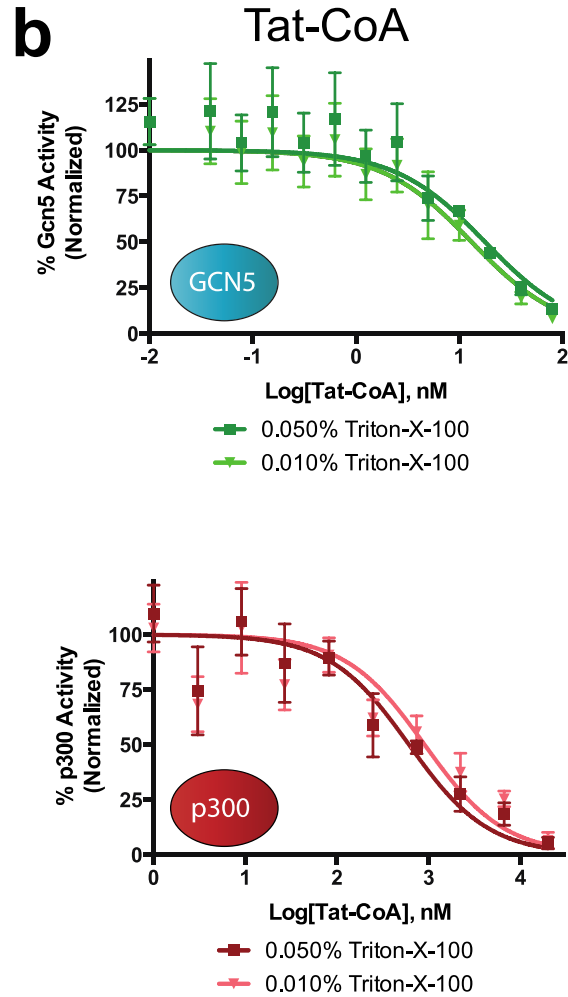
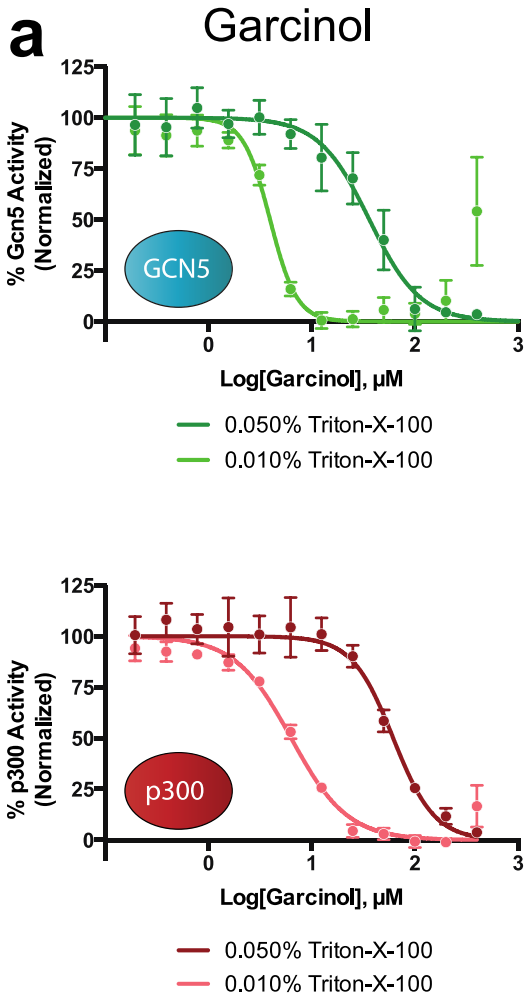


**Figure S7:** Detergent sensitivity of garcinol's inhibition of Gcn5 (top) and p300 (bottom). (b) Detergent sensitivity of Tat-CoA's inhibition of Gcn5 (top) and p300 (bottom).



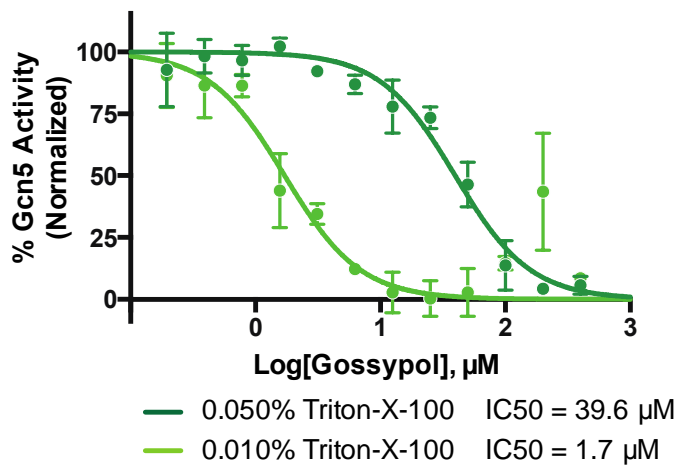


**Figure S8:** Detergent sensitivity of gossypol's inhibition of p300.

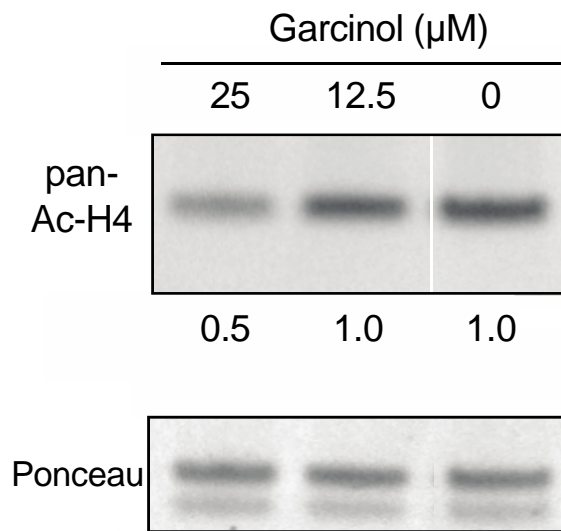
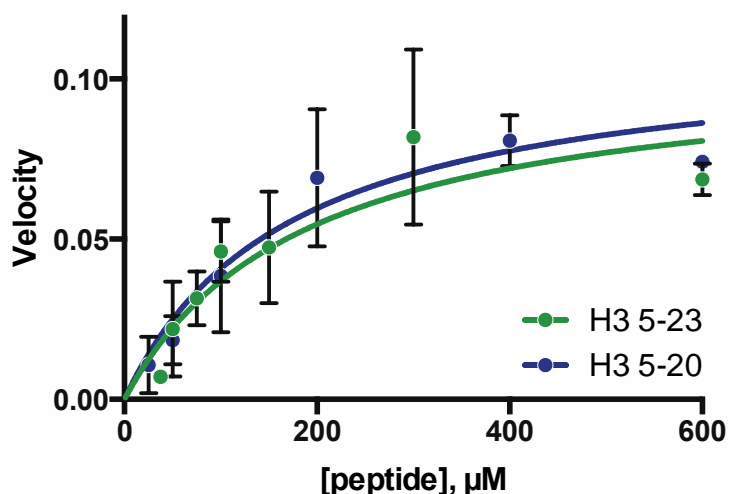


**Figure S9:** Effects of garcinol on histone acetylation in cells.

H4	Sequence
1-21	SGRGKGGKGLGKGGAKRHRKV (+8)
1-19	SGRGKGGKGLGKGGAKRHR (+7)
3-14	RGKGGKGLGKGG (+4)
3-11	RGKGGKGLG (+3)
4-11	GKGGKGLG (+2)
1-11	GGKGLG (+1)

H3	Sequence
1-20	ARTKQTARKSTGGKAPRKQL (+7)
5-23	TARKSTGGKAPRKQLATK (+6)
5-20	TARKSTGGKAPRKQL (+5)

**Table S1:** Sequence and charge of KAT substrate peptides used in this study. Positively charged residues are listed in red. All peptides were modified with an aminohexanoic acid-FITC linker at the N-terminus.



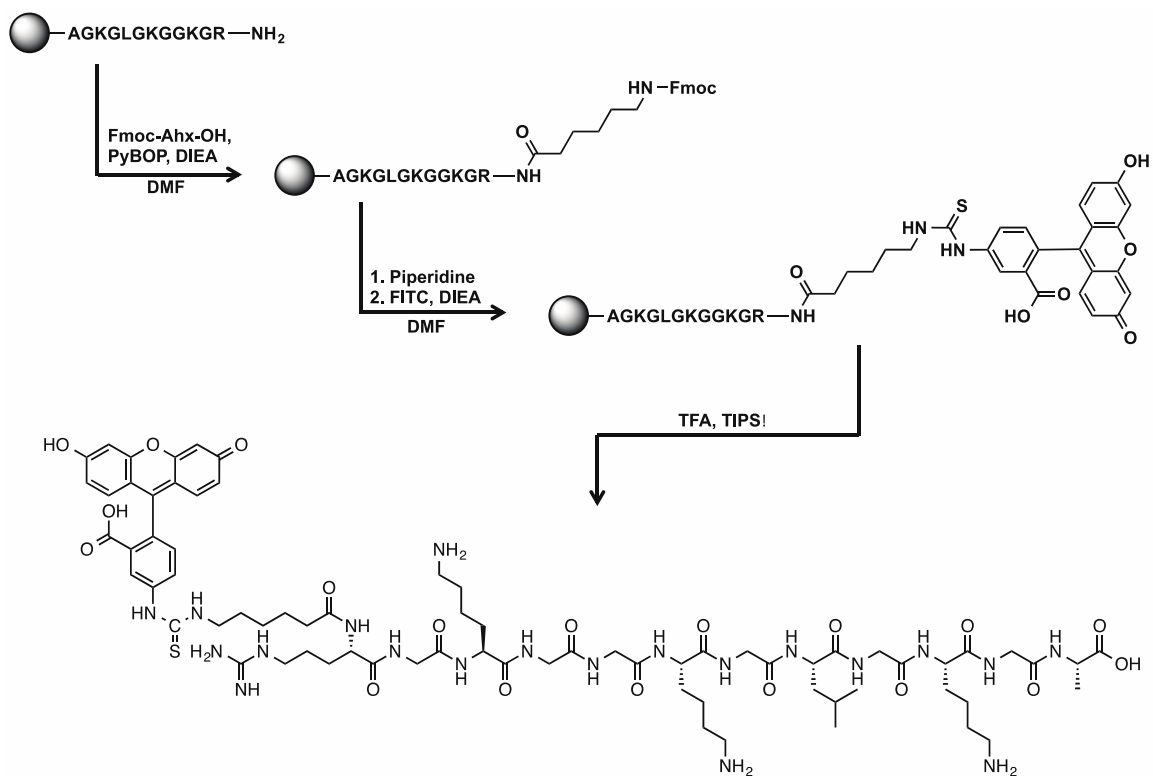
Michaelis-Menten plots for GCN5 comparing utilization of H3 5-23 and H3 5-20 peptide substrates. Plots represent rate of NADH production obtained from a coupled-enzyme assay (described below) in which GCN5 (187.5 nM) was incubated with variable concentrations of H3 5-23 and H3 5-20 peptide (18.75  $\mu$ M – 600  $\mu$ M) in the presence of AcCoA (60  $\mu$ M).

<b>a</b>	p300 Substrate	$K_m$ ( $\mu$ M)	$K_{cat}$ ( $s^{-1}$ )	$K_{cat}/K_m$ ( $s^{-1} M^{-1}$ )
	H4 1-19	$1.9 \pm 0.4$	$0.29 \pm 0.02$	$1.5 \times 10^5$
	H4 3-14	$8.3 \pm 1.4$	$0.38 \pm 0.01$	$4.6 \times 10^4$
	Ac-CoA	$1.2 \pm 0.2$	$0.26 \pm 0.01$	$2.1 \times 10^5$

<b>b</b>	GCN5 Substrate	$K_m$ ( $\mu$ M)	$K_{cat}$ ( $s^{-1}$ )	$K_{cat}/K_m$ ( $s^{-1} M^{-1}$ )
	H3 5-23	$187 \pm 69$	$0.56 \pm 0.09$	$3.0 \times 10^3$
	H3 5-20	$172 \pm 76$	$0.59 \pm 0.11$	$3.4 \times 10^3$
	Ac-CoA	$1.2 \pm 0.6$	$0.19 \pm 0.04$	$1.6 \times 10^5$

**Table S2:** Kinetic constants for (a) p300 and (b) Gcn5 with truncated peptide substrates (lacking Ahx-FITC label). Constants for p300 were previously reported.<sup>2</sup> GCN5 constants were calculated by fitting data obtained from coupled-enzyme assays<sup>1</sup> to the non-linear equation  $Y = (E_t \cdot K_{cat} \cdot [S]) / (K_m + [S])$ . Calculations were performed using Prism 6 (GraphPad) software.

**Table S3:** Percent inhibition of p300 and Gcn5 by each compound tested in model screen. (Provided as stand alone Excel File in Supplemental Information Section).



**Scheme S1:** General synthesis of FITC-labeled peptides.

### **Procedure for KAT-coupled enzyme assay**

KAT activity was measured by a previously reported coupled-enzyme assay.<sup>1</sup> This assay couples the production of CoA by KATs to the consumption of CoA and NAD<sup>+</sup> by  $\alpha$ -ketoglutarate dehydrogenase ( $\alpha$ -KGDH), which produces succinyl-CoA and NADH. The production of NADH can be continuously measured at 340 nm by ultraviolet-visible spectroscopy. Assays were performed in 150  $\mu$ L volumes containing 50 mM Bis-Tris, 50 mM Tris, 100 mM sodium acetate (TBA buffer, pH=7.5), 5 mM MgCl<sub>2</sub>, 1 mM DTT, 2.4 mM  $\alpha$ -ketoglutarate, 200  $\mu$ M thiamine pyrophosphate (TPP), 200  $\mu$ M NAD and 0.035 units of  $\alpha$ -KGDH (as defined by supplier), unlabeled histone H3/H4 peptide (25 to 600  $\mu$ M) and 187.5 nM GCN5 or 50 nM p300. Reactions were plated in 96-well plates and allowed to equilibrate at room temperature for 10 min. Reactions were initiated by addition of acetyl-CoA (final concentration = 0.313 to 5  $\mu$ M) and analyzed continuously for 5 min by measuring NADH production at 340 nm. GCN5-catalyzed reaction rates were background corrected by subtracting the rate of spontaneous formation of CoA (determined from reactions lacking KATs).

## General Synthetic Procedures

Chemicals were purchased from commercial sources (Sigma-Aldrich, Alfa Aesar, TCI America, and EMD) and used without further purification unless otherwise noted. Anhydrous solvents were prepared by passage over activated alumina. Automated peptide synthesis was carried out on an Applied Biosystems 433A Peptide Synthesizer. Peptide purification was carried out on an Agilent 1260 Infinity Quad pump HPLC using a Phenomenex Gemini (110 Å, 10µM) C18 column and a flow rate of 10 mL/min. Analytical LC/MS was performed using a Shimadzu LCMS-2020 Single Quadrupole utilizing a Kinetex 2.6 µm C18 100 Å (2.1 x 50 mm) column obtained from Phenomenex Inc. Analytical runs employed a gradient of 0→90% MeCN/0.1% aqueous formic acid over 4 minutes at a flow rate of 0.2 mL/min.

## Synthesis of fluorescent peptide substrates

Fluorescent H4 and H3 peptides were synthesized by automated peptide synthesis on Rink amide resin (0.2-0.5 mm scale, 0.68 mmol/g loading), using Fmoc-based chemistry. Amino acids were activated using HCTU (1eq, 0.45M solution in DMF), capped using acetic anhydride (5% in NMP), and deprotected using DBU (5% in piperidine). Following Fmoc-deprotection of the N-terminal amino acid, resin was removed from the automated peptide synthesizer and Fmoc-Ahx-OH (4 eq) and FITC (2 eq) were incorporated via manual coupling/deprotection in a glass reaction vessel. Reactions were monitored by Kaiser test. Following the final FITC coupling, peptides were treated with a cleavage solution (95% TFA, 2.5% H<sub>2</sub>O, 2.5% TIPS; 30 minutes) and purified *via* preparative reverse-phased HPLC using 0.1%TFA/H<sub>2</sub>O and MeCN. An exemplary gradient was as follows: 5 % MeCN (0→5 min), 5→50% MeCN (5→60 min), 50→95% MeCN (60-70 min; flush), 95→5% MeCN (70-75 min), 5% MeCN (75-80 min; reequilibration). Peptides were analyzed by LC-MS, lyophilized, and quantified by mass (unlabeled) or UV-Vis spectroscopy (FITC-labeled).



**Synthetic characterization data for fluorescent peptide substrates**

<b>N-term</b>	<b>Core</b>	<b>Sequence</b>	<b><i>m/z</i> expected</b>	<b><i>m/z</i> found</b>
FITC	H4(1-19)	SGRGKGGKGLGKGGAKRHR	1114.6 (+2)	1114.6 (+2)
FITC	H4(3-14)	RGKGGKGLGKGG	1587.6 (+1)	1587.1 (+1)
FITC	H4(3-11)	RGKGGKGLG	1331.5 (+1)	1331.1 (+1)
FITC	H4(4-11)	GKGGKGLG	1174.3 (+1)	1174.0 (+1)
FITC	H4(6-11)	GGKGLG	990.1 (+1)	990.0 (+1)
FITC	H3(5-23)	TARKSTGGKAPRKQLATK	633.0 (+4)	633.3 (+4)
FITC	H3(5-20)	TARKSTGGKAPRKQL	1114.6 (+2)	1114.6 (+2)
Ac	H3(5-23)	TARKSTGGKAPRKQLATK	1014.1 (+2)	1014.3 (+2)
Ac	H3(5-20)	TARKSTGGKAPRKQL	576.0 (+3)	576.5 (+3)

**References:**

1. Kim, Y.; Tanner, K. G.; Denu, J. *Anal. Biol.* 2000, 280, 308–314.
2. Thompson, P. R.; Kurooka H., Nakatani Y., Cole P. A. *J. Biol. Chem.* 2001, 276, 33721–33729.